Semarak Proceedings of Applied Sciences and Engineering Technology

Journal homepage:
https://semarakilmu.my/index.php/spaset/index
ISSN: 3083-9807

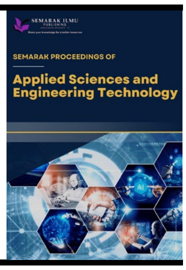

Exploring Flow Stability: Influence of Slip, Soret, and Dufour on Cu-Water Nanofluid over a Stretching/Shrinking Sheet

Najwa Najib[1,*], Norfifah Bachok[2], Nor Ashikin Abu Bakar[3], Nor Fadhilah Dzulkifli[4], Ahmad Fadly Nurullah Rasedee[1], Ioan Pop[5]

1 Faculty of Economics and Muamalat, Universiti Sains Islam Malaysia, Bandar Baru Nilai, Nilai 71800, Negeri Sembilan, Malaysia Department of Oil and Gas Engineering, Basrah University for Oil and Gas, Basrah, Iraq
2 Department of Mathematics and Institute for Mathematical Research, Universiti Putra Malaysia, 43400 UPM Serdang, Selangor, Malaysia
3 Institute of Engineering Mathematics,Universiti Malaysia Perlis, Kampus Pauh Putra,02600, Arau, Perlis, Malaysia
4 Kolej Pengajian Pengkomputeran Informatik dan Matematik, Universiti Teknologi MARA (UiTM) Cawangan Pahang, Kampus Jengka, 26400 Bandar Pusat Jengka, Pahang Darul Makmur, Malaysia
5 Department of Mathematics, Babeş-Bolyai University, 400084 Cluj-Napoca, Romania

ABSTRACT

Nanofluids have gained significant attention in industrial and engineering applications due to their enhanced thermal conductivity, making them suitable for cooling systems, heat exchangers, and electronic devices. Despite extensive research on boundary layer flow in nanofluids, the influence of thermodiffusion (Soret effect) and diffusion-thermo (Dufour effect) in the presence of second-order slip has not been thoroughly explored. This study aims to investigate the effects of second-order slip, Soret, and Dufour parameters on stagnation boundary layer flow over a stretching/shrinking sheet immersed in a Cu-water nanofluid. The primary objective is to analyze how these parameters influence skin friction, heat transfer, and mass transfer characteristics. The governing partial differential equations are transformed into ordinary differential equations using similarity transformations and numerically solved via the bvp4c solver in MATLAB. Results indicate that the presence of the first-order slip parameter broadens the solution region, whereas the second-order slip parameter narrows it. Additionally, the Soret effect enhances the heat transfer rate, while the Dufour effect increases mass transfer at the surface. The study also reveals the existence of dual solutions, necessitating a stability analysis to determine which solution is physically realizable. The findings provide valuable insights into optimizing nanofluid applications in industrial and engineering processes.

Keywords: Stagnation point flow; nanofluids; stretching/shrinking; second-order slip; Soret and Dufour effects; stability solutions

1. Introduction

Consideration of nanofluids in industrial processes and engineering fields such as cooling systems in electronic devices, heat exchangers, nuclear reactors and automotive cooling applications have become a great attraction nowadays. This is due to advantages of nanofluids which can enhance thermal conductivity up to two times by adding a small amount (<1% volume fraction) of nanoparticles in the fluid [1]. Nanofluids are also known as a based fluid that contains nanometer-sized particles (called as nanoparticles). Since water, ethylene-glycol and mineral oil has lower

* *Corresponding author.*
E-mail address: najwanajib@usim.edu.my

https://doi.org/10.37934/spaset.2.1.1531

thermal conductivity that is not sufficient to act as a cooling agent and hence nanofluid is one way to address this matter. Many works have been investigated involving nanofluids in boundary layer flow which can be found in [2-7]. Recent advancements in nanofluid research have expanded into hybrid nanofluids and complex flow conditions. Studies such as the Darcy-Forchheimer flow of hybrid carbon nanotube-based nanofluid over a permeable stretching/shrinking curved surface have provided insight into fluid dynamics over non-planar geometries, showcasing the impact of permeability and nanoparticle volume fraction on flow characteristics [8]. Additionally, the magnetohydrodynamic (MHD) flow of Williamson hybrid nanofluids over a non-linear shrinking sheet with viscous dissipation and Joule heating extends the understanding of heat transfer in non-Newtonian hybrid nanofluids [9]. These studies highlight the transition from conventional nanofluids to more complex hybrid systems, paving the way for future applications in thermal management and energy systems.

Furthermore, thermodiffusion (Soret effect) and diffusion-thermo (Dufour effect) play a crucial role in heat and mass transfer, especially in the presence of concentration gradients and temperature variations. These effects are significant in applications such as the fabrication of semiconductor devices, polymer separation, and enhanced oil recovery. By adding chemical species to the surface of the fluid, then the density may vary at the surrounding fluid, therefore Soret and Dufour effects of heat and mass cannot be negligible. The application of the thermodiffusion in industrial applications can be found in fabrication of semiconductor devices in molten metal and semiconductor mixtures, separation of polymers and DNA as well as in optimum oil recovery from hydrocarbon reservoirs, see Eslamian [10]. The first research on existence and development of Soret and Dufour effects was done by Kafoussias and Williams [11] where they consider both effects on vertical plate with temperature dependent viscosity. Elbade *et al.,* [12] has extended the previous work in power law non-Newtonian fluid. Some investigation has been carried out to study Soret and Dufour effects passing through permeable plate, when the plate is partially heated and when the plate is oscillated in horizontal cavity [13-15]. Instead of studying the effects on different plates, Hayat *et al.,* [16] and Pal *et al.,* [17] considered the thermodiffusion and diffusion-thermo in Maxwell fluid and nanofluid, respectively. The consideration of Soret and Dufour effects on MHD boundary layer flow has been presented in the works by Hamid *et al.,* [18], Subhakar *et al.,* [19] and Reddy *et al.,* [20]. More, some work on the effects of Soret and Dufour has been done when the fluid is immersed in porous medium in boundary layer [21-24]. Very recently, the influence of magnetohydrodynamic orientation on Soret and Dufour effects within inclined, corrugated triangular cavities containing non-Newtonian fluids, underscoring the impacts of magnetic alignment, cavity inclination, and fluid rheology on convective transport dynamics [25].

One of the key factors influencing nanofluid behavior in boundary layer flows is the slip condition at the surface. While classical no-slip boundary conditions have been widely assumed, practical situations such as rarefied gas flows and microfluidic applications necessitate considering velocity slip effects. The first-order slip model has been extensively studied; however, recent findings suggest that the second-order slip model can more accurately describe the flow dynamics, particularly in high-Knudsen-number regimes. Hence, Wu [26] have formulated a second order slip model for rarefied gas flows from kinetic theory. The proposed second order slip model was used by Fang and Aziz [27] and Fang *et al.,* [28]. Recently, Mabood and Mastroberardino [29], Mabood and Das [30] and Mabood *et al.,* [31] had applied the slip model in their works on MHD boundary layer on a melting plate. The study on unsteady cases in different fluids such as in micropolar and nanofluid were investigated by Narayana and Gangadhar [32] and Alam *et al.,* [33]. Wu [34] again analyzed the mass suction on viscous gas flows over a stretching/shrinking sheet. A numerical analysis of MHD ternary hybrid nanofluid flow past a permeable stretching/shrinking surface with slip effect have been recently studied in [35].

The focus of this paper is to extend the work by Bachok *et al.*, [5] when thermodiffusion (Soret effect) and diffusion-thermo (Dufour effect) is taken into consideration with presence of second order slip at the boundary condition. The stability solutions are implemented into this study due to dual solutions obtained. Therefore, we carry out numerical computation to verify either first or second solution is stable and physically realizable. The pioneer research on stability solutions was done by Merkin [36]. Very recently, many works on stability solutions can be found in Bachok *et al.,* [37], Ismail *et al.,* [38] and Najib *et al.,* [39,40].

The current literature lacks a comprehensive investigation of the combined effects of second-order slip, Soret, and Dufour on stagnation boundary layer flow in nanofluids. Understanding these interactions is crucial for optimizing thermal and mass transfer processes in advanced industrial applications. This study aims to address this gap by numerically analyzing the impact of these parameters on skin friction, heat transfer, and mass transfer characteristics over a stretching/shrinking sheet immersed in Cu-water nanofluid. Additionally, stability analysis will be conducted to determine which of the dual solutions is physically realizable, providing further insights into nanofluid dynamics. Apart from that, the present study focusses on nanofluid, hence the results obtain can be set as a benchmark to investigate advance fluid such as hybrid and ternary nanofluid.

2. Methodology
2.1 Basic Equations

Consider the flow of incompressible nanofluid in the region $y > 0$ driven by a stretching/shrinking surface located at $y = 0$ with a fixed stagnation point at $x = 0$ in the presence of Soret and Dufour effects as well as slip effect at the wall. It is assumed that the free stream and stretching/shrinking velocity are assumed in the linear form $U_e = ax$ and $U_w = bx$, respectively where a and b are constant with $a > 0$. Note that $b > 0$ and $b < 0$ correspond to stretching and shrinking sheet, respectively. Under these conditions the boundary layer equations are:

$$\frac{\partial u}{\partial x} + \frac{\partial v}{\partial y} = 0 \tag{1}$$

$$\frac{\partial u}{\partial t} + u\frac{\partial u}{\partial x} + v\frac{\partial u}{\partial y} = U_e\frac{dU_e}{dx} + \frac{\mu_{nf}}{\rho_{nf}}\frac{\partial^2 u}{\partial y^2} \tag{2}$$

$$\frac{\partial T}{\partial t} + u\frac{\partial T}{\partial x} + v\frac{\partial T}{\partial y} = \alpha_{nf}\frac{\partial^2 T}{\partial y^2} + \frac{D_m K_T}{c_s c_p}\frac{\partial^2 C}{\partial y^2} \tag{3}$$

$$\frac{\partial C}{\partial t} + u\frac{\partial C}{\partial x} + v\frac{\partial C}{\partial y} = D_m\frac{\partial^2 C}{\partial y^2} + \frac{D_m K_T}{T_m}\frac{\partial^2 T}{\partial y^2} \tag{4}$$

along with the initial and boundary conditions:

$$\begin{aligned} &t < 0: u = v = 0, \quad T = T_\infty, \quad C = C_\infty \quad &&\text{for any } x, y \\ &t \ge 0: u = U_w + U_{slip},\ v = 0,\ T = T_f,\ C = C_f \quad &&\text{at} \quad y = 0 \\ &\qquad u \to U_e, \quad T \to T_\infty, \quad C \to C_\infty, \quad &&\text{as} \quad y \to \infty \end{aligned} \tag{5}$$

where u and v are the velocity components along $x-$ and $y-$ axes, respectively, T is the nanofluid temperature. U_{slip} is the slip velocity at the wall. The Wu's slip velocity model (valid for arbitrary Knudsen numbers, *Kn*) is used in this paper and is given as follows [25]:

$$\begin{aligned} U_{slip} &= \frac{2}{3}\left(\frac{3-\alpha l^3}{\alpha} - \frac{3}{2}\frac{1-l^2}{K_n}\right)\lambda\frac{\partial u}{\partial y} - \frac{1}{4}\left(l^4 + \frac{2}{K_n^{\,2}}\left(1-l^2\right)\right)\lambda^2\frac{\partial^2 u}{\partial y^2} \\ &= A\frac{\partial u}{\partial y} + B\frac{\partial^2 u}{\partial y^2} \end{aligned} \tag{6}$$

where A and B are constants, K_n is Knudsen number, $l = \min(1/K_n, 1)$, α is the momentum accommodation coefficient with $0 \le \alpha \le 1$, and λ is the molecular mean free path. Based on the definition of l, it is seen that for any given value of K_n, we have $0 \le l \le 1$. Since the molecular mean free path λ is always positive it results in that B is a negative number.

Further, α_{nf} is the effective thermal diffusivity of the nanofluid, μ_{nf} is the dynamic viscosity of the nanofluid and ρ_{nf} is the density of the nanofluid, which given in Table 1 (Oztop and Abu-Nada, [2]). The physical characteristics of the nanofluid are given by:

$$\begin{aligned} &\rho_{nf} = (1-\varphi)\rho_f + \varphi\rho_s, \quad \alpha_{nf} = \frac{k_{nf}}{(\rho C_p)_{nf}}, \quad \mu_{nf} = \frac{\mu_f}{(1-\varphi)^{2.5}} \\ &(\rho C_p)_{nf} = (1-\varphi)(\rho C_p)_f + \varphi(\rho C_p)_s, \quad \frac{k_{nf}}{k_f} = \frac{(k_s+2k_f) - 2\varphi(k_f-k_s)}{(k_s+2k_f) + \varphi(k_f-k_s)} \end{aligned} \tag{7}$$

where φ is the nanoparticle volume fraction, k_{nf} is the effective thermal conductivity of the nanofluid and C_p is the specific heat at constant pressure.

Table 1
Thermophysical properties of fluid and nanoparticles [2].

Physical properties	Fluid phase (water)	Cu
C_p (J/kg K)	4179	385
ρ (kg/m^3)	997.1	8933
k (W/mK)	0.613	400
$\alpha \times 10^7$ (m^2/s)	1.47	11163.1
$\beta \times 10^{-5}$ (1/K)	21	1.67

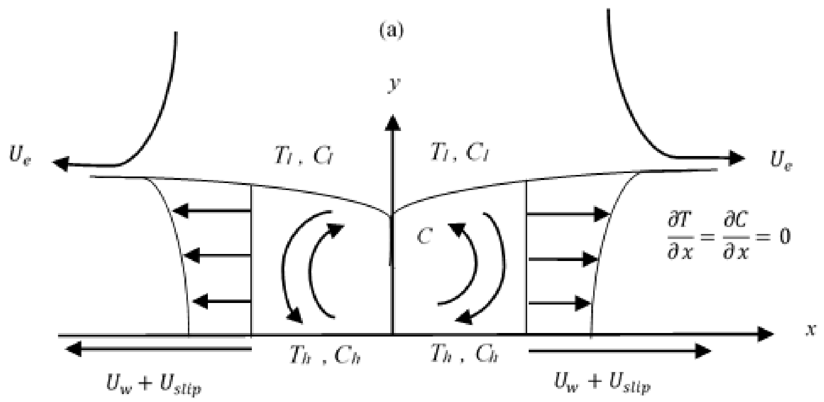

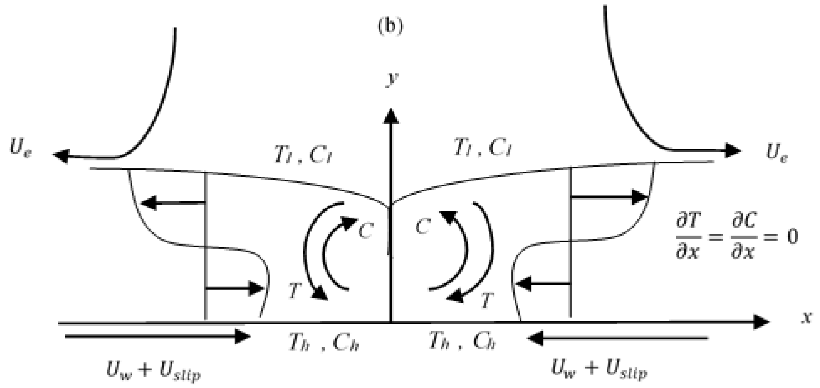

Fig. 1. Physical model and coordinate system (a) stretching sheet and (b) shrinking sheet

2.1 Steady-State Solution $\left(\partial / \partial t = 0\right)$

Introducing the following similarity transformation.

$$\psi=\sqrt{a\nu_f}\,xf(\eta), \quad \theta(\eta)=\frac{T-T_\infty}{T_f-T_\infty}, \quad \phi(\eta)=\frac{C-C_\infty}{C_f-C_\infty}, \quad \eta=\sqrt{\frac{a}{\nu_f}}y, \tag{8}$$

where η is the similarity variable and ψ is the stream function defined as $u=\partial\psi/\partial y$ and $v=-\partial\psi/\partial x$, which automatically satisfied Eq. (1). Substitute the similarity variables (8) into Eqs. (2) to (4) we obtain the following ordinary (similarity) differential equations.

$$\frac{1}{(1-\varphi)^{2.5}(1-\varphi+\varphi\rho_s/\rho_f)}f'''+ff''-f'^2+1=0 \tag{9}$$

$$\frac{k_{nf}}{k_f}\theta''+\Pr(1-\varphi+\varphi(\rho c_p)_s/(\rho c_p)_f)\left(f\theta'+Df\phi''\right)=0 \tag{10}$$

$$\phi''+Sc\left(f\phi'+Sr\theta''\right)=0 \tag{11}$$

subject to the boundary conditions:

$$\begin{aligned} &f(0)=0, \quad f'(0)=\varepsilon+\sigma f''(0)+\delta f'''(0), \quad \theta(0)=1, \quad \phi(0)=1 \\ &f'(\eta)\to 1, \quad \theta(\eta)\to 0, \quad \phi(\eta)\to 0 \quad \text{as} \quad \eta\to\infty \end{aligned} \tag{12}$$

In the above equations, primes denote the differentiation with respect to η. Following Mukhopadhyay and Andersson [41], we take $A=\sigma\sqrt{\nu_f/a}$ and $B=\delta(\nu_f/a)$ with $\sigma>0$ being the first velocity slip and $\delta<0$ is the second velocity slip parameters (see Fang *et al.,* [27]). Here $\Pr$ is the Prandt number, Sc is the Schmidt number, Sr is the Soret number, Df is the Dufour number and ε is the velocity ratio parameter which are defined as:

$$\Pr = \frac{\nu_f}{\alpha_f}, \quad Sc = \frac{\nu_f}{D_m}, \quad Sr = \frac{D_m K_T}{\nu_f T_m}\frac{T_f - T_\infty}{C_f - C_\infty}, \quad Df = \frac{D_m K_T}{\nu_f c_s c_p}\frac{C_f - C_\infty}{T_f - T_\infty}, \quad \varepsilon = \frac{b}{a}, \tag{13}$$

where $\varepsilon > 0$ for stretching and $\varepsilon < 0$ for shrinking.

The physical quantities of practical interest are the local skin friction coefficients C_f, local Nusselt number Nu_x and local Sherwood number Sh_x which are defined as:

$$C_f = \frac{\tau_w}{\rho_f U_e^{\,2}}, \quad Nu_x = \frac{x q_w}{k_f (T_f - T_\infty)}, \quad Sh_x = \frac{x q_m}{D_m (C_f - C_\infty)}, \tag{14}$$

where τ_w is the skin friction or the shear stresses on the stretching/shrinking sheet, q_w is the heat flux from the surface of the plate and q_m is the mass flux from the surface of the plate, which are given by:

$$\tau_w = \mu_{nf}\left(\frac{\partial u}{\partial y}\right)_{y=0}, \quad q_w = -k_{nf}\left(\frac{\partial T}{\partial y}\right)_{y=0}, \quad q_m = -D_m\left(\frac{\partial C}{\partial y}\right)_{y=0}, \tag{15}$$

Using Eq. (8) in Eq. (14) and Eq. (15), we obtain:

$$\left(\mathrm{Re}_x\right)^{1/2} C_f = \frac{1}{(1-\varphi)^{2.5}} f''(0), \quad \mathrm{Re}_x^{-1/2} Nu_x = -\frac{k_{nf}}{k_f}\theta'(0), \quad \mathrm{Re}_x^{-1/2} Sh_x = -\phi'(0) \tag{16}$$

where $\mathrm{Re}_x = a x^2 / \nu_f$ is the local Reynolds number.

2.3 Stability Equations

Roşca and Pop [42] and Weidman *et al.,* [43] have shown for the forced convection boundary layer flow past a permeable flat plate and, respectively, for the mixed convection flow past a vertical flat plate that the lower branch solutions are unstable (not realizable physically), while the upper branch solutions are stable (physically realizable). We test these features by considering the unsteady Eqs. (2)-(3). Thus, we introduce the new dimensionless time variable $\tau = at$. The use of τ is associated with an initial value problem and is consistent with the question of which solution will be obtained in practice (physically realizable). Using the variables τ and (8), we have:

$$\eta = \sqrt{\frac{a}{\nu_f}}, \quad \psi = \sqrt{a\nu_f}\, x f(\eta,\tau), \quad \theta(\eta,\tau) = \frac{T - T_\infty}{T_f - T_\infty}, \quad \phi(\eta,\tau) = \frac{C - C_\infty}{C_f - C_\infty}, \quad \tau = at \tag{17}$$

so that Eqs. (2) and (3) can be written as:

$$\frac{1}{(1-\varphi)^{2.5}(1-\varphi+\varphi\rho_s/\rho_f)}\frac{\partial^3 f}{\partial \eta^3} + f\frac{\partial^2 f}{\partial \eta^2} - \left(\frac{\partial f}{\partial \eta}\right)^2 + 1 - \frac{\partial^2 f}{\partial \eta \partial \tau} = 0 \tag{18}$$

$$\frac{k_{nf}}{k_f}\frac{\partial^2\theta}{\partial\eta^2}+\Pr(1-\varphi+\varphi(\rho c_p)_s/(\rho c_p)_f)\left(f\frac{\partial\theta}{\partial\eta}+Df\frac{\partial^2\phi}{\partial\eta^2}-\frac{\partial\theta}{\partial\tau}\right)=0 \quad (19)$$

$$\frac{\partial^2\phi}{\partial\eta^2}+Sc\left(f\frac{\partial\phi}{\partial\eta}+Sr\frac{\partial^2\theta}{\partial\eta^2}-\frac{\partial\phi}{\partial\tau}\right)=0 \quad (20)$$

Subject to the boundary conditions:

$$\begin{aligned}&F_0(0)=0,\quad F_0'(0)=\sigma F_0''(0)+\delta F_0'''(0),\quad G_0(0)=0,\quad H_0(0)=0,\\&F_0'(\eta)\to 0,\quad G_0(\eta)\to 0,\quad H_0(\eta)\to 0\quad \text{as}\quad \eta\to\infty\end{aligned} \quad (21)$$

It should be mentioned that for particular values of $\varepsilon,\sigma,\delta,\Pr,Sr,Df,Sc$ and φ the stability of the corresponding steady flow solution $f_0(\eta)$, $\theta_0(\eta)$ and $\phi_0(\eta)$, is determined by the smallest eigenvalue γ. According to Harris *et al.,* [44], the range of possible eigenvalues can be determined by relaxing a boundary condition either on $F_0(\eta)$, $G_0(\eta)$ or $H_0(\eta)$.

3. Methodology

The system of nonlinear ordinary differential Eqs. (9) – (11) along with respective boundary condition Eq. (12). The numerical solutions are obtained using MATLAB's bvp4c solver, ensuring accuracy through comparison with prior validated studies. The stability analysis follows the approach outlined by Merkin [36], determining the physically realizable solutions. Several values of selected parameters namely first order slip parameter σ, second order slip parameter δ, nanoparticle volume fraction parameter φ, Soret effect parameter *Sr* as well as Dufour effect parameter *Df* have been analyzed to investigate the flow behavior on the boundary layer. Table 2 and 3 depict the comparison of numerical results with previous research. As stated in the tables, our numerical results are in a very good agreement with the previous papers and hence give us confidence that our numerical results obtained, and figures are correct.

Table 2
Values of $f''(0)$ for some values of ε when $\sigma=\delta=Sr=Df=0\ \ \varphi=0.1$

ε	Bachok *et al.,* [5]		Present Value	
	First Solution	Second Solution	First Solution	Second Solution
2	-2.217106		-2.217106	
1	0		0	
0.5	0.837940		0.837940	
0	1.447977		1.447977	
-0.5	1.757032		1.757032	
-1	1.561022	0	1.561022	0
-1.15	1.271347	0.137095	1.271347	0.137095
-1.2	1.095419	0.274479	1.095419	0.274479
-1.2465	0.686379	0.651161	0.686382	0.651157

Table 3
Values of $C_f \mathrm{Re}_x^{1/2}$ for some values of ε and $\varphi = 0.1$ when $\sigma = \delta = Sr = Df = 0$

ε	Yacob *et al.,* [9]	Bachok *et al.,* [5]	Present results
-0.5	1.8843	2.2865	2.2865
0		1.8843	1.8843
0.5		1.0904	1.0904

The skin friction coefficient, temperature gradient and also concentration gradient are plotted for some values of first and second-order slip parameter (σ and δ) in Figures 2-4. In the absent of slip parameters $(\sigma = \delta = 0)$, the unique solution is occurred from $\varepsilon > -1$, dual solutions happen in between $\varepsilon_c \le \varepsilon \le -1$ and no solution is mark when $\varepsilon < \varepsilon_c$ (see Figure 1). On the other situation when we consider first and second-order slip parameter at the boundary, the region of dual solutions become larger from ε critical (ε_c) up to -0.9 $(\varepsilon_c \le \varepsilon \le -0.9)$(see Figure 2). In the absent of first order slip parameter $(\sigma = 0)$, the dual solutions are admitted to happen from ε_c up to -0.5 $(\varepsilon_c \le \varepsilon \le -0.5)$ when we increased the second-order slip parameter $|\delta|$. However, the presence of first-order slip parameter σ causes the region of solutions become larger compared to only second-order slip δ is considered (the critical values in Figure 3 are larger than in Figure 4). Therefore, the second order slip parameter $(\delta \ne 0)$ leads to narrowing the region of solutions while the first order slip parameter $(\sigma \ne 0)$ result in broadening the region of solutions. In the presence of slip parameters at the boundary cause decrease the surface shear stress and mass transfer at the surface due to slippery surface (reduced the holdings between nanoparticles). However, heat transfer rate is increasing as the first and second order slip parameter (σ, δ) is increasing.

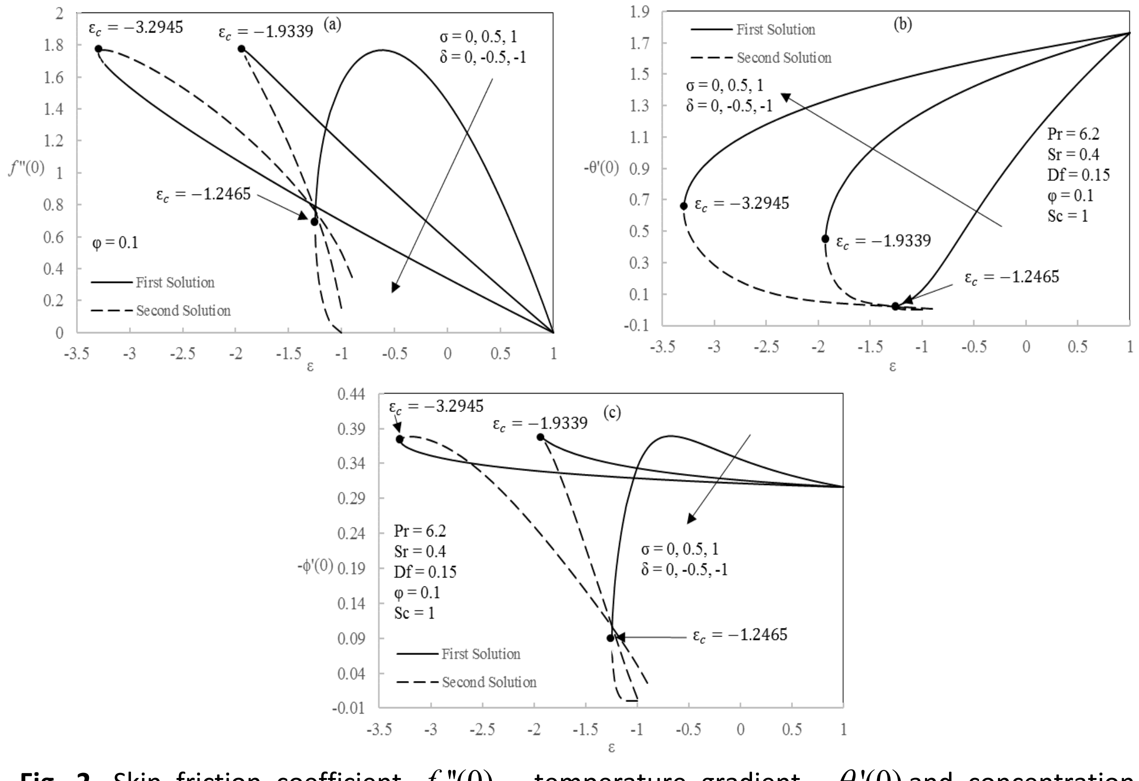

Fig. 2. Skin friction coefficient $f''(0)$, temperature gradient $-\theta'(0)$ and concentration gradient $-\phi'(0)$ vs. ε for several values of σ and δ.

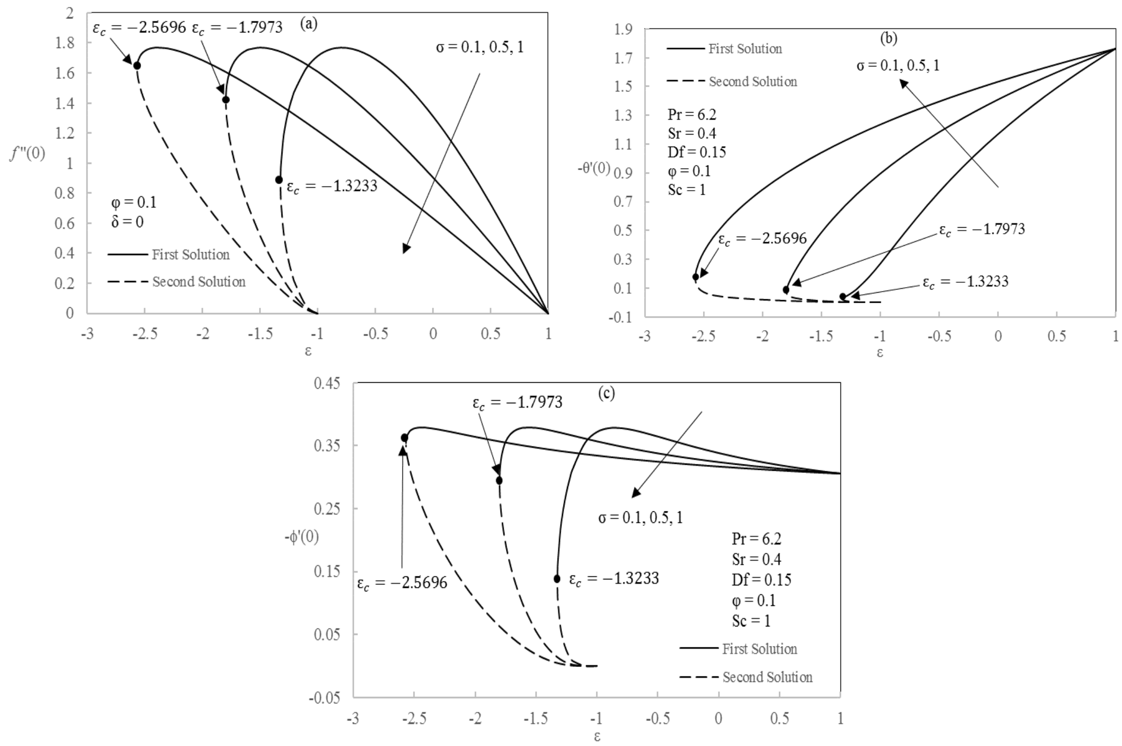

Fig. 3. Skin friction coefficient $f''(0)$, temperature gradient $-\theta'(0)$ and concentration gradient $-\phi'(0)$ vs. ε for several values of σ

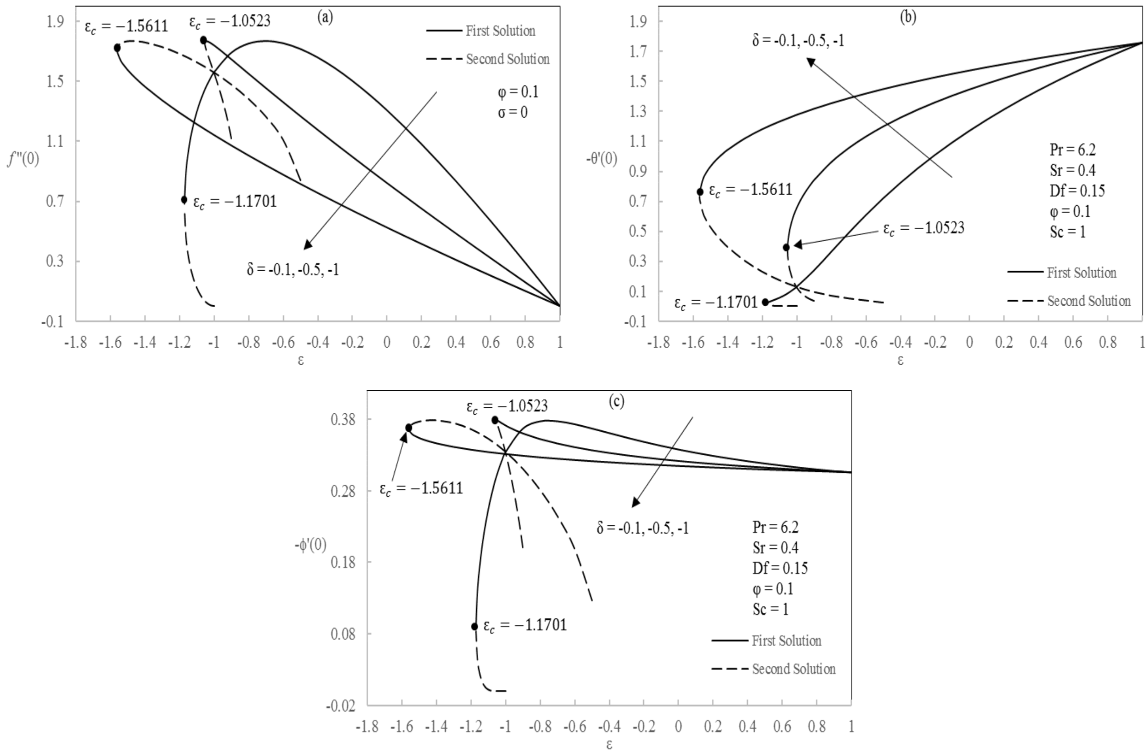

Fig. 4. Skin friction coefficient $f''(0)$, temperature gradient $-\theta'(0)$ and concentration gradient $-\phi'(0)$ vs. ε for several values of δ

Figure 5 indicates the skin friction coefficient, temperature gradient and concentration gradient for some values of nanoparticle volume fraction between 0 to 0.2 $(0 \le \varphi \le 0.2)$. From these figures, we want to discuss how the number of nanoparticles will affect the skin friction coefficient, heat as well as mass transfer at the surface. The skin friction coefficient and mass transfer are increasing when we increase the nanoparticle volume fraction while the increase of nanoparticle volume fraction causes decrease the heat transfer at the surface. Since nanoparticles enhanced the thermal conductivity of the fluid, higher values of thermal conductivity are accompanied by higher values of thermal diffusivity. Hence high value of thermal diffusivity leads to drop in the temperature gradient or heat transfer rate at the surface (see Sharma and Ishak [45]).

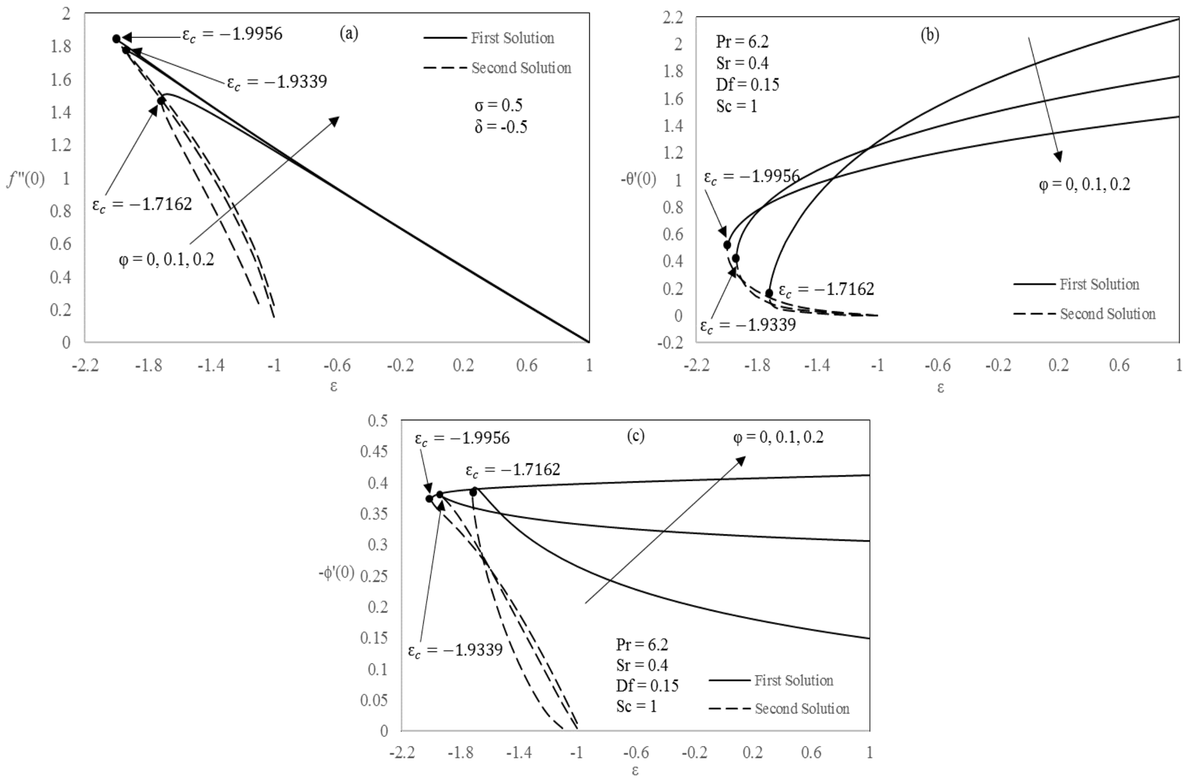

Fig. 5. Skin friction coefficient $f''(0)$, temperature gradient $-\theta'(0)$ and concentration gradient $-\phi'(0)$ vs. ε for several values of ϕ

The effects of Soret and Dufour are presented in Figures 6 and 7. In Figure 6 we have fixed the value of Dufour effect *Df* is equal to 0.15 $(Df = 0.15)$ where we are only focusing on different values of Soret effects *Sr*. The heat transfer is increasing when we increase the values of *Sr* but the other situation is observed where mass transfer is decreasing as *Sr* increased. Soret effect is referred to as thermal diffusion (thermodiffusion) where the particles (in this case we consider nanoparticle) are diffused from higher temperature to lower temperature due to the mass flux. The different effects on Dufour *Df* can be seen in Figure 7 where Soret effect is taken to be 0.15 $(Sr = 0.15)$. The reverse observation has been reported where the heat transfer is decreasing when we increased *Df* meanwhile the mass transfer is increasing as *Df* is increasing. This is because Dufour effect is the reverse phenomenon of Soret effect called diffusion-thermo. The nanoparticles diffused from higher concentration to lower concentration due to energy (heat) flux. The findings of this study have significant practical implications in industrial and engineering applications. The enhanced understanding of slip and thermodiffusion effects in nanofluid flow can be applied in designing efficient cooling systems, such as heat exchangers, microelectronics cooling, and biomedical thermal therapy. The ability to manipulate heat and mass transfer properties through slip parameters and nanoparticle concentration provides a pathway for optimizing energy efficiency in industrial processes. Future research should focus on experimental validation of the theoretical results, exploring hybrid nanofluids, and extending the analysis to three-dimensional flow conditions for more comprehensive modeling.

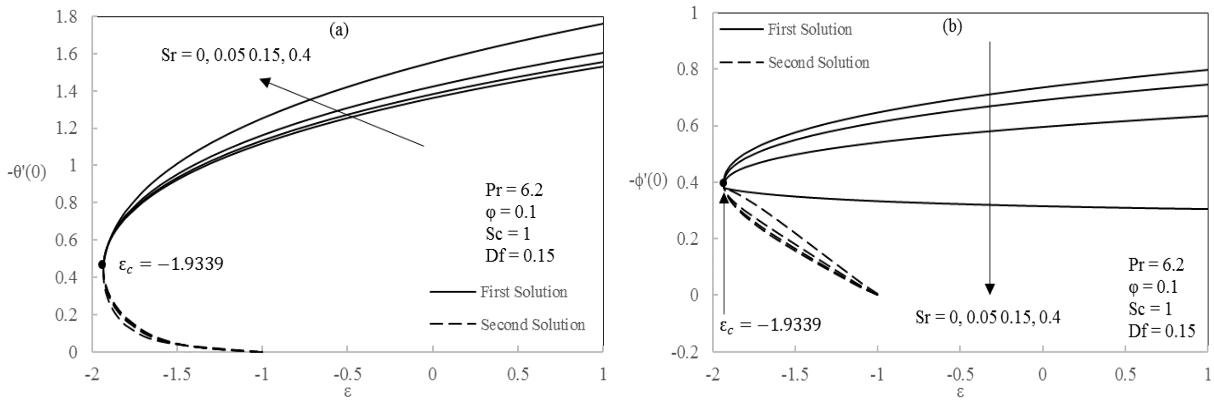

Fig. 6. Temperature gradient $-\theta'(0)$ and concentration gradient $-\phi'(0)$ vs. ε for several values of Sr

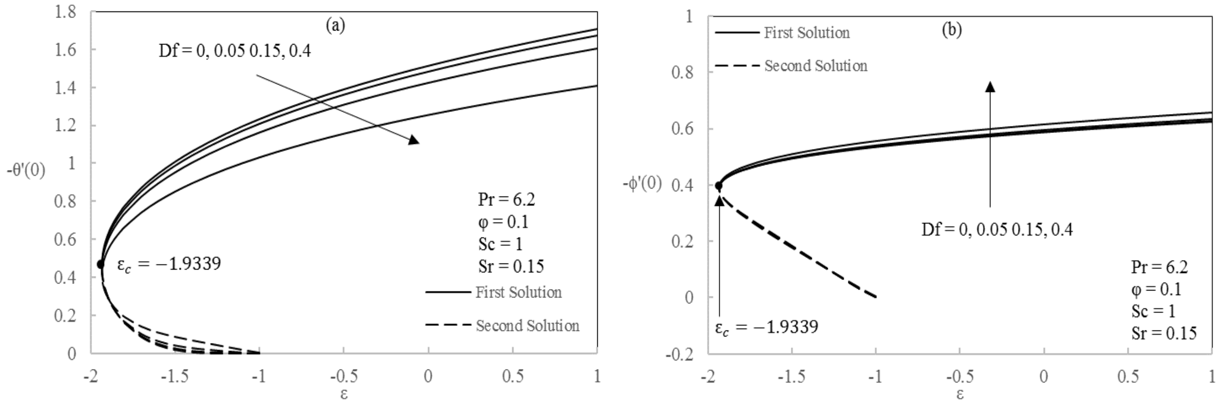

Fig. 7. Temperature gradient $-\theta'(0)$ and concentration gradient $-\phi'(0)$ vs. ε for several values of Df

The dual velocity, temperature as well as concentration profiles have been shown graphically in Figures 8-11 to support our numerical results and the Figures 2-7 obtained are correct. All presented profiles satisfy the far field boundary conditions Eq. (12) by obeying the behavior or characteristic of the flow asymptotically. Moreover, the boundary layer thickness for the second solution is always larger than the first solution.

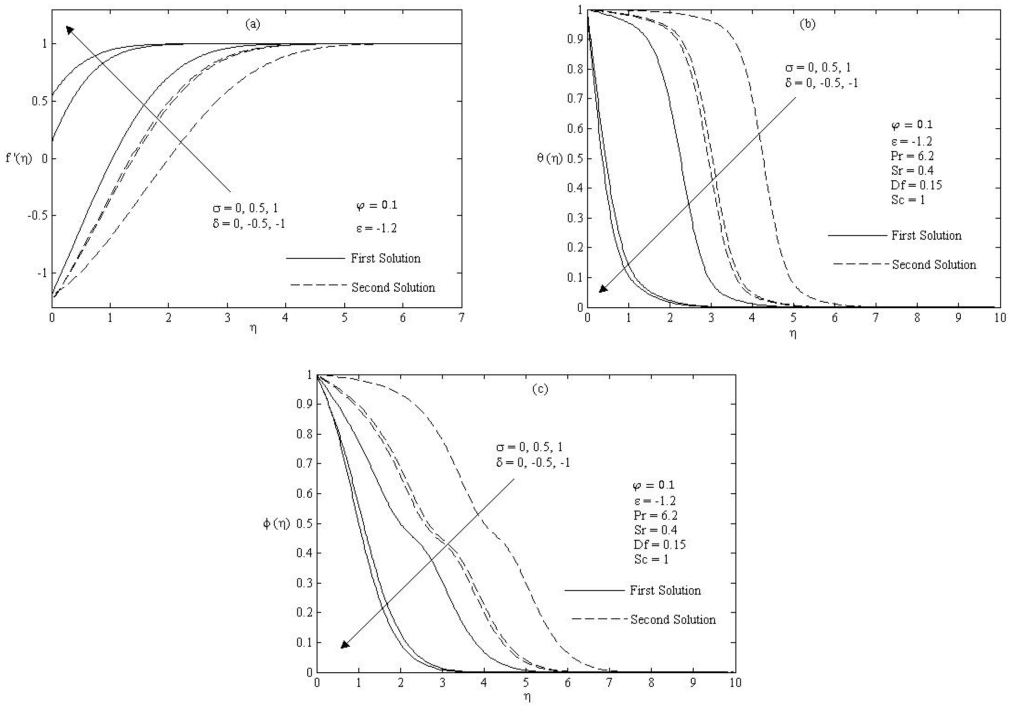

Fig. 8. Dual velocity profile $f'(\eta)$, temperature profile $\theta(\eta)$ and concentration profile $\phi(\eta)$ for several values of σ and δ

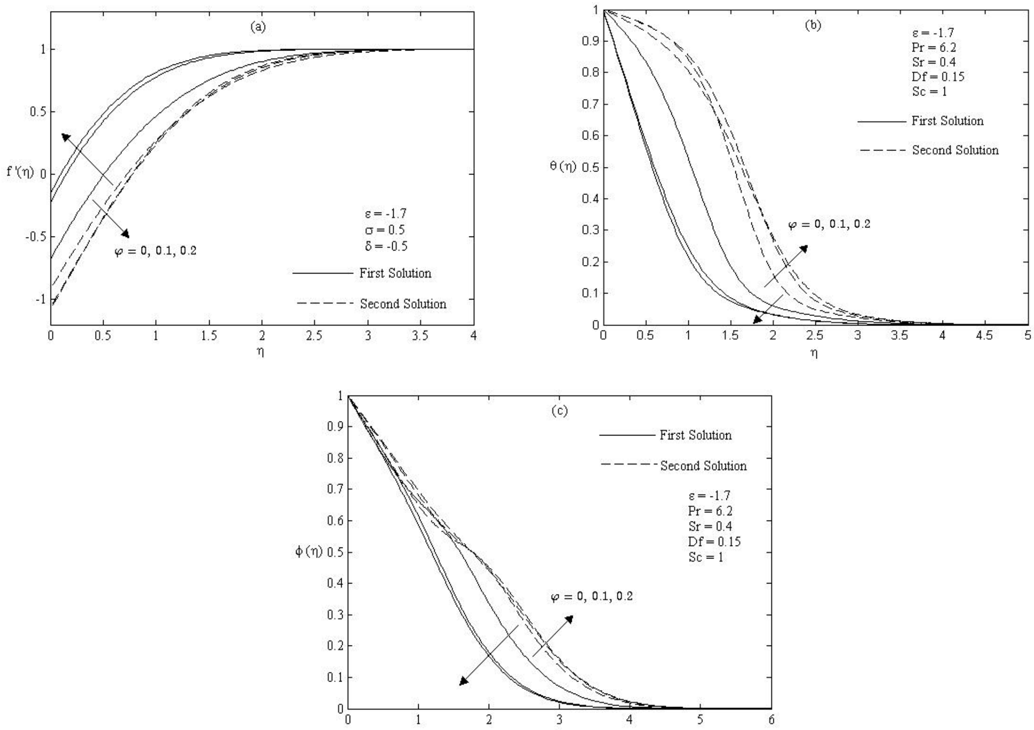

Fig. 9. Dual velocity profile $f'(\eta)$, temperature profile $\theta(\eta)$ and concentration profile $\phi(\eta)$ for several values of ϕ.

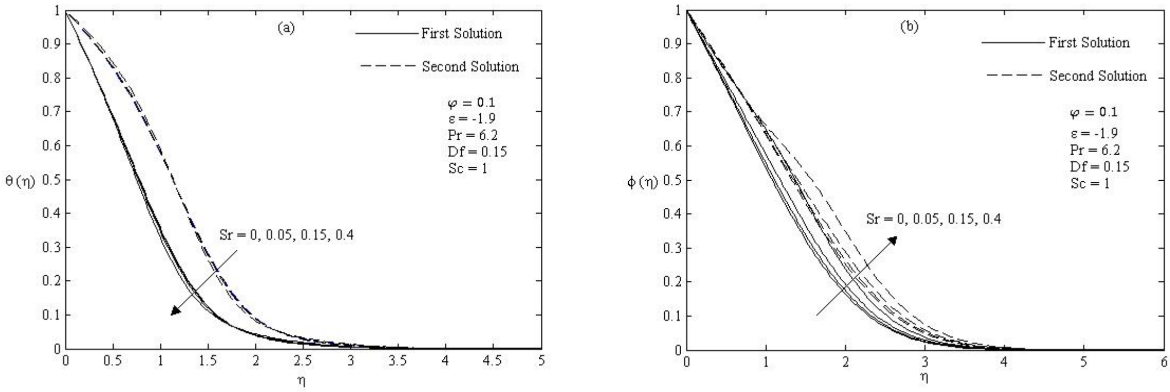

Fig. 10. Dual temperature profile $\theta(\eta)$ and concentration profile $\phi(\eta)$ for several values of *Sr*

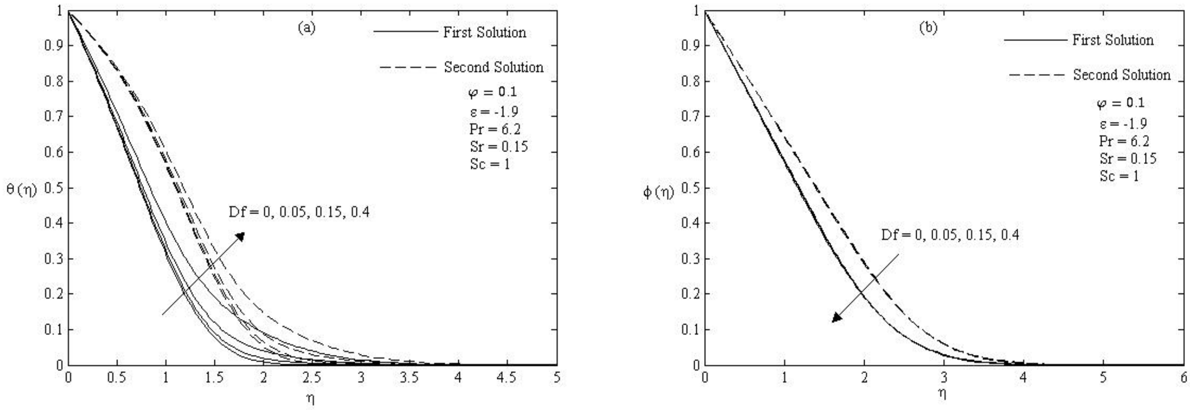

Fig. 11. Dual temperature profile $\theta(\eta)$ and concentration profile $\phi(\eta)$ for several values of *Df*

The smallest eigenvalues γ for some values of ε in various values of first and second order slip parameter (σ,δ) are presented in Table 4. As we can see that the eigenvalue γ will approaching zero ($\gamma \to 0$) when the selected value ε is nearer to the critical point ε_c. From our observation, γ is positive (stable solution) for the first solution and negative (unstable solution) for the second solution. The solution is said to be in stable state when there only slight disturbance on the flow system that does not affect the flow characteristics while the unstable solution is stated when there existed initial growth of disturbance that affect the flow system. Thus, the first solution is said as a stable solution and hence can be realized physically but the second solution is corresponding to unstable solution and at once their physical meaning cannot be realized physically.

The stability analysis performed in this study is not only a numerical exercise but holds substantial physical significance. In practical applications, flow stability determines whether a specific solution can be observed in real-world scenarios. For instance, in industrial processes involving nanofluids, a stable solution corresponds to a predictable and controllable flow regime, crucial for designing efficient cooling and heat transfer systems. Unstable solutions, on the other hand, indicate sensitivity to disturbances, leading to unpredictable behaviour that may compromise system performance. The confirmation that the first solution is stable implies that engineers and scientists can rely on this solution when implementing nanofluid-based technologies. Furthermore, the results provide a deeper understanding of flow bifurcation phenomena, essential for optimizing boundary conditions in advanced thermal applications such as biomedical fluid dynamics and energy storage systems.

Future experimental studies should validate these theoretical findings to further confirm their applicability in real-world scenarios.

Table 4
Smallest eigenvalues γ for selected values of ε with different σ and δ when ϕ = 0.1

σ	δ	ε	First Solution	Second Solution
0	0	-1.2465	0.0230	-0.0229
		-1.246	0.0622	-0.0614
		-1.24	0.2121	-0.2036
		-1.2	0.5780	-0.5172
		-1.1	1.0463	-0.8437
0.5	-0.5	-1.9339	0.0150	-0.0150
		-1.933	0.0593	-0.0592
		-1.93	0.1205	-0.1201
		-1.9	0.3538	-0.3502
		-1.8	0.7043	-0.6894
1	-1	-3.2945	0.0078	-0.0078
		-3.294	0.0321	-0.0321
		-3.29	0.0939	-0.0938
		-3.2	0.4300	-0.4266
		-3.1	0.6173	-0.6102

4. Conclusions

We have studied numerically the effects of second-order slip, Soret as well as Dufour effect on stagnation boundary layer flow over a stretching/shrinking sheet immersed in Cu-water nanofluid using Tiwari and Das model and we also performed the stability solutions to verify which solutions is stable. We found that:

i. the solutions happen in dual when the plate is shrinking $(\varepsilon < 0)$.
ii. The consideration of first and second-order slip are affected the flow characteristics where the region of solutions become narrow when the second-order slip is presented $(\delta \neq 0)$ while in the presence of first-order slip $(\sigma \neq 0)$ the region of solutions become broader.
iii. increasing the value of nanoparticle volume fraction φ leads to increase the surface shear stress and mass transfer rate at the surface while decreasing in heat transfer rate.
iv. Larger Soret effect leads to increase the heat transfer rate but cause the mass transfer rate to decrease at the surface.
v. Larger Dufour effect cause the heat transfer rate to decrease but somehow leads the mass transfer rate to increase at the surface.
vi. the first solution is in stable state while the second solution is not. Therefore the physical meaning of the first solution is realize physically whereas the physical meaning of the second solution cannot be realized physically.

Acknowledgement
This research was not funded by any grant.

References

[1] Choi, S. US, and Jeffrey A. Eastman. *Enhancing thermal conductivity of fluids with nanoparticles*. No. ANL/MSD/CP-84938; CONF-951135-29. Argonne National Lab.(ANL), Argonne, IL (United States), 1995.

[2] Oztop, Hakan F., and Eiyad Abu-Nada. "Numerical study of natural convection in partially heated rectangular enclosures filled with nanofluids." *International journal of heat and fluid flow* 29, no. 5 (2008): 1326-1336. https://doi.org/10.1016/j.ijheatfluidflow.2008.04.009

[3] Salleh, S. N. A., N. Bachok, and N. M. Arifin. "Rotating boundary layer flow due to a permeable exponentially shrinking sheet in nanofluid." *International Journal of Pure and Applied Mathematics* 112, no. 1 (2017): 57-69. https://doi.org/10.12732/ijpam.v112i1.4

[4] Kardri, Mahani Ahmad, Norfifah Bachok, Norihan Md Arifin, and Fadzilah Md Ali. "Boundary layer flow and heat transfer over a stretching cylinder in a copper-water nanofluid." In *AIP Conference Proceedings*, vol. 1795, no. 1. AIP Publishing, 2017. https://doi.org/10.1063/1.4972156

[5] Bachok, Norfifah, Anuar Ishak, and Ioan Pop. "Stagnation-point flow over a stretching." *Nanoscale research letters* 6, no. 1 (2011): 1-10. https://doi.org/10.1186/1556-276X-6-623

[6] Roşca, Natalia C., and Ioan Pop. "Axisymmetric rotational stagnation point flow impinging radially a permeable stretching/shrinking surface in a nanofluid using Tiwari and Das model." *Scientific reports* 7, no. 1 (2017): 40299. https://doi.org/10.1038/srep40299

[7] Omar, Noor Syamimi, Norfifah Bachok, and Norihan Md Arifin. "Stagnation point flow over a stretching or shrinking cylinder in a copper-water nanofluid." *Indian Journal of Science and Technology* 8, no. 31 (2015): 1-7. https://doi.org/10.17485/ijst/2015/v8i31/85405

[8] Anuar, Nur Syazana, Nur Adilah Liyana Aladdin, and Ioan Pop. "Darcy-Forchheimer Flow of Hybrid Carbon Nanotube over a Permeable Stretching/Shrinking Curved Surface." *Journal of Advanced Research in Fluid Mechanics and Thermal Sciences* 126 (2):73-85. https://doi.org/10.37934/arfmts.126.2.7385

[9] Mokhtar, Masyfu'ah, Abdul Rahman Mohd Kasim, Iskandar Waini, Nur Syahidah Nordin, Siti Farah Haryatie Mohd Kanafiah, and Adeosun Adeshina Taofeeq. "Magnetohydrodynamic of Williamson Hybrid Nanofluids Flow over a Non-Linear Shrinking Sheet with Viscous Dissipation and Joule Heating." *Semarak Engineering Journal* 7, no. 1 (2024): 31-47. https://doi.org/10.37934/sej.7.1.3147

[10] Eslamian, Morteza. "Advances in thermodiffusion and thermophoresis (Soret effect) in liquid mixtures." *Frontiers in Heat and Mass Transfer (FHMT)* 2, no. 4 (2012). https://doi.org/10.5098/hmt.v2.4.3001

[11] Kafoussias, N. G., and E. W. Williams. "Thermal-diffusion and diffusion-thermo effects on mixed free-forced convective and mass transfer boundary layer flow with temperature dependent viscosity." *International Journal of Engineering Science* 33, no. 9 (1995): 1369-1384. https://doi.org/10.1016/0020-7225(94)00132-4

[12] Eldabe, Nabil T., A. G. El-Saka, and Ashraf Fouad. "Thermal-diffusion and diffusion-thermo effects on mixed free-forced convection and mass transfer boundary layer flow for non-Newtonian fluid with temperature dependent viscosity." *Applied mathematics and computation* 152, no. 3 (2004): 867-883. https://doi.org/10.1016/S0096-3003(03)00603-9

[13] Alam, M. S., and M. M. Rahman. "Dufour and Soret effects on mixed convection flow past a vertical porous flat plate with variable suction." *Nonlinear Analysis: Modelling and Control* 11, no. 1 (2006): 3-12. https://doi.org/10.15388/NA.2006.11.1.14761

[14] Nithyadevi, N., and Ruey-Jen Yang. "Double diffusive natural convection in a partially heated enclosure with Soret and Dufour effects." *International Journal of Heat and Fluid Flow* 30, no. 5 (2009): 902-910. https://doi.org/10.1016/j.ijheatfluidflow.2009.04.001

[15] Wang, Jin, Mo Yang, Ya-Ling He, and Yuwen Zhang. "Oscillatory double-diffusive convection in a horizontal cavity with Soret and Dufour effects." *International Journal of Thermal Sciences* 106 (2016): 57-69. https://doi.org/10.1016/j.ijthermalsci.2016.03.012

[16] Hayat, Tasawar, Meraj Mustafa, and Said Mesloub. "Mixed convection boundary layer flow over a stretching surface filled with a Maxwell fluid in presence of Soret and Dufour effects." *Zeitschrift für Naturforschung A* 65, no. 5 (2010): 401-410. https://doi.org/10.1515/zna-2010-0505

[17] Pal, Dulal, Gopinath Mandal, and Kuppalapalle Vajravalu. "Soret and Dufour effects on MHD convective–radiative heat and mass transfer of nanofluids over a vertical non-linear stretching/shrinking sheet." *Applied Mathematics and Computation* 287 (2016): 184-200. https://doi.org/10.1016/j.amc.2016.04.037

[18] Hamid, Rohana Abdul, W. M. K. A. Wan Zaimi, Norihan Md Arifin, Nor Ashikin Abu Bakar, and Biliana Bidin. "Thermal diffusion and diffusion thermo effects on MHD thermosolutal Marangoni convection boundary layer flow over a permeable surface." *Journal of Applied mathematics* 2012, no. 1 (2012): 750939. https://doi.org/10.1155/2012/750939

[19] Subhakar, M. J., K. Gangadhar, and N. Bhaskar Reddy. "Soret and Dufour effects on MHD convective flow of heat and mass transfer over a moving non-isothermal vertical plate with heat generation/absorption." *Advances in Applied Science Research* 3, no. 5 (2012): 3165-3184.

[20] Reddy, G. Jithender, R. Srinivasa Raju, P. Manideep, and J. Anand Rao. "Thermal diffusion and diffusion thermo effects on unsteady MHD fluid flow past a moving vertical plate embedded in porous medium in the presence of Hall current and rotating system." *Transactions of A. Razmadze Mathematical Institute* 170, no. 2 (2016): 243-265. https://doi.org/10.1016/j.trmi.2016.07.001

[21] Moorthy, M. B. K., T. Kannan, and K. Senthilvadivu. "Soret and Dufour effects on natural convection heat and mass transfer flow past a horizontal surface in a porous medium with variable viscosity." *WSEAS Transactions on Heat and Mass Transfer* 8, no. 4 (2013): 74-83.

[22] Balla, Chandra Shekar, and Kishan Naikoti. "Soret and Dufour effects on free convective heat and solute transfer in fluid saturated inclined porous cavity." *Engineering Science and Technology, an International Journal* 18, no. 4 (2015): 543-554. https://doi.org/10.1016/j.jestch.2015.04.001

[23] Srinivasacharya, D., B. Mallikarjuna, and R. Bhuvanavijaya. "Soret and Dufour effects on mixed convection along a vertical wavy surface in a porous medium with variable properties." *Ain Shams Engineering Journal* 6, no. 2 (2015): 553-564. https://doi.org/10.1016/j.asej.2014.11.007

[24] Reddy, P. Sudarsana, and Ali J. Chamkha. "Soret and Dufour effects on MHD convective flow of Al2O3–water and TiO2–water nanofluids past a stretching sheet in porous media with heat generation/absorption." *Advanced Powder Technology* 27, no. 4 (2016): 1207-1218. https://doi.org/10.1016/j.apt.2016.04.005

[25] Shah, Syed Saqib. "Magnetohydrodynamic orientation effects on Soret and Dufour phenomena in inclined corrugated triangular cavities with non-Newtonian fluids." *International Communications in Heat and Mass Transfer* 160 (2025): 108366. https://doi.org/10.1016/j.icheatmasstransfer.2024.108366

[26] Wu, Lin. "A slip model for rarefied gas flows at arbitrary Knudsen number." *Applied Physics Letters* 93, no. 25 (2008). https://doi.org/10.1063/1.3052923

[27] Fang, Tiegang, and Abdul Aziz. "Viscous flow with second-order slip velocity over a stretching sheet." *Zeitschrift für Naturforschung A* 65, no. 12 (2010): 1087-1092. https://doi.org/10.1515/zna-2010-1212

[28] Fang, Tiegang, Shanshan Yao, Ji Zhang, and Abdul Aziz. "Viscous flow over a shrinking sheet with a second order slip flow model." *Communications in Nonlinear Science and Numerical Simulation* 15, no. 7 (2010): 1831-1842. https://doi.org/10.1016/j.cnsns.2009.07.017

[29] Mabood, Fazle, and Antonio Mastroberardino. "Melting heat transfer on MHD convective flow of a nanofluid over a stretching sheet with viscous dissipation and second order slip." *Journal of the Taiwan Institute of Chemical Engineers* 57 (2015): 62-68. https://doi.org/10.1016/j.jtice.2015.05.020

[30] Mabood, F., and K. Das. "Melting heat transfer on hydromagnetic flow of a nanofluid over a stretching sheet with radiation and second-order slip." *The European Physical Journal Plus* 131 (2016): 1-12. https://doi.org/10.1140/epjp/i2016-16003-1

[31] Mabood, F., A. Shafiq, T. Hayat, and S. Abelman. "Radiation effects on stagnation point flow with melting heat transfer and second order slip." *Results in Physics* 7 (2017): 31-42. https://doi.org/10.1016/j.rinp.2016.11.051

[32] Narayana, K. Lakshmi, and K. Gangadhar. "Second order slip flow of a MHD micropolar fluid over an unsteady stretching surface." *Advances in Applied Science Research* 6, no. 8 (2015): 224-241.

[33] Alam, M. S., M. M. Haque, and M. J. Uddin. "Convective flow of nanofluid along a permeable stretching/shrinking wedge with second order slip using Buongiorno's mathematical model." *International Journal of Advanced in Applied Mathematics and Mechanics* 3, no. 3 (2016): 79-91. https://doi.org/10.18280/mmep.030101

[34] Wu, Lin. "Mass transfer induced slip effect on viscous gas flows above a shrinking/stretching sheet." *International Journal of Heat and Mass Transfer* 93 (2016): 17-22. https://doi.org/10.1016/j.ijheatmasstransfer.2015.09.080

[35] Ouyang, Yun, Md Faisal Md Basir, Kohilavani Naganthran, and Ioan Pop. "Numerical analysis of MHD ternary nanofluid flow past a permeable stretching/shrinking sheet with velocity slip." *Alexandria Engineering Journal* 116 (2025): 427-438. https://doi.org/10.1016/j.aej.2024.12.089

[36] Merkin, J. H. "On dual solutions occurring in mixed convection in a porous medium." *Journal of engineering Mathematics* 20, no. 2 (1986): 171-179. https://doi.org/10.1007/BF00042775

[37] Bachok, Norfifah, Najwa Najib, Norihan Md Arifin, and Norazak Senu. "Stability of dual solutions in boundary layer flow and heat transfer on a moving plate in a copper-water nanofluid with slip effect." WSEAS Transactions on Fluid Mechanics 11, no. 19 (2016): 151-158.

[38] Ismail, Nurul Syuhada, Norihan Md Arifin, Norfifah Bachok, and Norhasimah Mahiddin. "Stagnation-point flow and heat transfer over an exponentially shrinking sheet: A stability analysis." In *AIP Conference Proceedings*, vol. 1739, no. 1. AIP Publishing, 2016. https://doi.org/10.1063/1.4952503

[39] Najib, Najwa, Norfifah Bachok, and Norihan Md Arifin. "Stability of dual solutions in boundary layer flow and heat transfer over an exponentially shrinking cylinder." *Indian Journal of Science and Technology* 9, no. 48 (2016): 1-6. https://doi.org/10.17485/ijst/2016/v9i48/97740

[40] Najib, Najwa, Norfifah Bachok, Norihan Md Arifin, and Norazak Senu. "Boundary layer flow and heat transfer of nanofluids over a moving plate with partial slip and thermal convective boundary condition: Stability analysis." *International Journal of Mechanics* 11, no. 1 (2017): 18-24.

[41] Mukhopadhyay, Swati, and Helge I. Andersson. "Effects of slip and heat transfer analysis of flow over an unsteady stretching surface." *Heat and Mass Transfer* 45 (2009): 1447-1452. https://doi.org/10.1007/s00231-009-0516-7

[42] Roşca, Alin V., and Ioan Pop. "Flow and heat transfer over a vertical permeable stretching/shrinking sheet with a second order slip." *International Journal of Heat and Mass Transfer* 60 (2013): 355-364. https://doi.org/10.1016/j.ijheatmasstransfer.2012.12.028

[43] Weidman, P. D., D. G. Kubitschek, and A. M. J. Davis. "The effect of transpiration on self-similar boundary layer flow over moving surfaces." *International journal of engineering science* 44, no. 11-12 (2006): 730-737. https://doi.org/10.1016/j.ijengsci.2006.04.005

[44] Harris, S. D., D. B. Ingham, and I. Pop. "Mixed convection boundary-layer flow near the stagnation point on a vertical surface in a porous medium: Brinkman model with slip." *Transport in Porous Media* 77 (2009): 267-285. https://doi.org/10.1007/s11242-008-9309-6

[45] Sharma, Rajesh, Anuar Ishak, and I. Pop. "Second order slip flow of cu-water nanofluid over a stretching sheet with heat transfer." *WSEAS Trans. Fluid Mech* 9 (2014): 26-33.